Vol. 23, No. 3(2024) Poly24316
Revista Mexicana de Ingeniería Química

Dosage of monomers in a polymerization reaction

Dosificación de monómeros en una reacción de polimerización

D. Guzmán-Lucero, J.F. Palomeque-Santiago, A. Vega-Paz, J. Guzmán-Pantoja, N. V. Likhanova, F.J. Guevara-Rodríguez*

Dirección de Investigación, Instituto Mexicano del Petróleo, Eje Central Lázaro Cárdenas 152, Ciudad de México, 07730, México.

Received: April 23, 2024; Accepted: May 18, 2024

Abstract

A model is proposed to estimate the dosage rate of monomers in a polymerization reaction. The model consists of a bimodal Gamma probability distribution function for describing the conversion velocity of monomers in a flask polymerization reaction (laboratory scale). The function of conversion percentage of monomers (the integral of the conversion velocity of monomers) is correlated with the experimental data. From this function, the conversion percentage of monomers is developed for a polymerization reaction, where monomers are added with a suitable dosage rate. The dosage rate of monomers is determined from a minimization procedure applied to the mean square deviation between the conversion percentage of the fast and slow monomers. In this way, the dosage rate of monomers is estimated to define the polymerization experiment on micro-plant scale. From these experiments, the resulting polymeric product (with 1 *L* or 5 *L* scale) is homogeneous and without residual monomers.
Keywords: Terpolymers, synthesis, Gamma distribution, dosage rate, micro plant.

Resumen

Se propone un modelo para estimar la tasa de dosificación de monómeros en una reacción de polimerización. El modelo se construye con una función de distribución de probabilidad Gamma bimodal para describir la velocidad de conversión de los monómeros en una reacción de polimerización en un recipiente (escala de laboratorio). La función de porcentaje de conversión de los monómeros (la integral de la velocidad de conversión de los monómeros) se correlaciona con los datos experimentales. A partir de esta función, se desarrolla el porcentaje de conversión de los monómeros para una reacción de polimerización en la que se añaden monómeros con una tasa de dosificación adecuada. La tasa de dosificación de los monómeros se determina a partir de un procedimiento de minimización aplicado a la desviación cuadrática media entre el porcentaje de conversión de los monómeros rápidos y lentos. De esta manera, se estima la tasa de dosificación de los monómeros para definir el experimento de polimerización a escala de micro planta. A partir de esos experimentos, el producto polimérico resultante (con una escala de 1 L o 5 L) es homogéneo y sin monómeros residuales.
Palabras clave: Terpolímeros, síntesis, distribución Gamma, tasa de dosificación, micro planta.

* *Corresponding author. E-mail*: fguevara@imp.mx;
https://doi.org/10.24275/rmiq/Poly24316
ISSN:1665-2738, *issn-e*: 2395-8472

1 Introduction

Researchers study polymeric reactions due to the wide diversity of high-value synthetic products for cosmetics, biomaterials, pharmaceuticals, coatings, wastewater treatment, and oil recovery, among many other industrial areas (Bailey, 2000), (Jaeger, 2010), (Williams, 2007), (Gromov, 1994), (Palomeque, 2022), (Cortés, 2011), (Martínez, 2007). There are two main branches in the classification of polymerization reactions, namely, condensation and addition reactions. In the first one, the polymer molecule and secondary products are formed simultaneously; in the second one, the monomer molecule becomes a polymer segment, however, in this case, an initiator is required in the addition polymerization reaction (Carraher, 2013). This work is focused on the addition polymerization reaction in aqueous solution. In this technique, the monomer and initiator are dissolved in water and the polymer is formed in solution. At the end of the reaction, the polymer can be recovered by precipitation or lyophilization. Polymers such as polyacrylic acid are commonly made by solution polymerization (Mark, 1999), (Ohara, 2011).

Controlled polymerization reactions result in polymers with desired molecular weight, molecular weight distribution and structural and physical properties. To achieve this objective, it is essential that factors such as (1) monomer conversion rates and reaction rates, (2) relationship of the reaction parameters with the molecular weight and distribution, and (3) reaction mechanism of the initiation, propagation, and termination steps be analyzed (Buback, 1990), (Ye, 2002), (Ray, 1999). All these issues are tackled by using the concepts of propagation (κ_p) and termination (κ_t) rate coefficients, which are functions of the temperature, pressure, chain length, monomer concentration, ionization degree, and ionic strength, i.e. of the enormous complexity of radical polymerizations in aqueous solution (Hutchinson, 1998), (Barner, 2017), (Buback, 2023). However, most works are devoted to the study of polymeric systems with one or two monomers, since terpolymer systems have a high degree of complexity (Meyer, 2003), (Santanakrishnan, 2010), (Preusser, 2016), (Bazaldua, 2023). As for the propagation and termination rate coefficients, they are determined from polymerization reactions on laboratory scale, but if scaling up to micro-plant level is considered, then, the chemical process has major viscosity changes and mass and heat transfer phenomena. Therefore, the polymerization reaction on micro-plant scale must be treated in a different way from that on lab scale. In particular, the propagation and termination rates must change, and these changes are not obvious (Meyer, 2003). Furthermore, the competition between different monomers in a polymerization reaction mixture on micro-plant scale is present. In this case, the differences regarding the conversion velocity of monomers constitute the main problem, and monomer dosage could be a solution, notwithstanding, the final product is affected by the monomer dosage rate and addition order of reactants, and these issues are not well understood (Vasile, 2015), (López, 2020). In the present work, a polymerization reaction using three monomers is analyzed on the lab and micro-plant scales. The reaction of monomers is analyzed by measuring the conversion of monomers and their time derivative. At this point, the conversion velocity of monomers is modeled by using the probability Gamma distribution function. Thus, the model is designed to describe the conversion at lab level, but in the next step, the model is extended to the micro-plant scale by using the monomer dosage rate procedure. The conversion of monomers (with dosage) is then modeled by using a convolution as a superposition of the conversion of monomers on lab scale, but at different initial times and weighted by the velocity of monomers added to the system.

2 Monomer conversion

2.1 *Lab scale*

The polymerization solution of the monomers acrylamide (AM), vinyl pyrrolidone (VP), and vinyl butyl imidazolium (VBIM) at 35:35:30 mol% was prepared in a three-neck flask using deaerated water under vacuum; nitrogen was introduced and maintained during the reaction. The temperature was set at 50 ºC and V50 was used as initiator. Samples were taken at different times, and a small amount of a hydroquinone solution was added to stop the reaction. Finally, ^{1}H-NMR analysis (Bruker 600 MHz spectrometer with Avance III as interface) was performed to determine the monomer conversion.

2.2 *Mathematical adjustment*

The conversion data derived from the polymerization experiment for each monomer in the mixture are described by

$$p_\alpha(t) = \int_0^t v_\alpha(\tau)\, d\tau \tag{1}$$

where $\alpha \in \{\text{AM, VP, VBIM}\}$ is the monomer label. The function p_α is the monomer-α conversion percentage at time t, meanwhile, v_α is the conversion velocity of monomers and is modeled with the N-

modal probability density function, namely.

$$v_\alpha(t) = 100\% \times \sum_{i=1}^{N} \omega_{\alpha i}\, \rho_{\alpha i}(t) \tag{2}$$

where $\omega_{\alpha i}$ is the fraction of the probability density function $\rho_{\alpha i}$ in a multimodal distribution and is normalized as $\omega_{\alpha 1} + \omega_{\alpha 2} + \cdots + \omega_{\alpha N} = 1$. In a polymerization reaction, the conversion velocity of monomers exhibits one or more dynamic regimes, thus this behavior is described by a multimodal distribution. However, in this work, a bimodal distribution is only considered, *i.e.*, $N = 2$. Regarding the probability density function ($\rho_{\alpha i}$ in min^{-1}), it is rewritten as

$$\rho_{\alpha i}(t) = \lambda_{\alpha i}\, \rho\left(\lambda_{\alpha i}(t - t_{\alpha i})\right) \tag{3}$$

where $\lambda_{\alpha i}$ is a positive parameter that expands or contracts the domain of function ρ, meanwhile $t_{\alpha i}$ is a non-negative-time-displacement parameter, and the probability density function is taken from the Gamma distribution function, namely

$$\rho(t) = \begin{cases} 0, & t \le 0; \\ t^{z-1} e^{-t}/\Gamma(z) & 0 < t, \end{cases} \tag{4}$$

where Γ is the Gamma function (Abramowitz, 1972)

$$\Gamma(z) = \int_0^\infty t^{z-1} e^{-t}\, dt. \tag{5}$$

The argument z, in the Gamma function is another parameter, but its value is fixed to $z = 5/2$ to have a smooth and continuous transition at the initial time, *i.e.*, $\rho(0) = 0$ and $\dot{\rho}(0) = 0$ (where $\dot{\rho}$ is the time derivative of ρ). In this case, the Gamma function has the value $\Gamma(z) = 3\sqrt{\pi}/4$, and the conversion function is

$$p_\alpha(t) = 100\% \times \sum_{i=1}^{N} \omega_{\alpha i} \left(erf\left(\sqrt{u_{\alpha i}}\right) - \sqrt{\frac{u_{\alpha i}}{\pi}} \left(\frac{4}{3}\, u_{\alpha i} + 2\right) e^{-u_{\alpha i}} \right) \tag{6}$$

where $u_{\alpha i}$ is the function

$$u_{\alpha i}(t) = \begin{cases} 0 & t \le t_{\alpha i}; \\ \lambda_{\alpha i}\ (\, t - t_{\alpha i}\,) & t_{\alpha i} < t, \end{cases} \tag{7}$$

and erf in Equation (6) is the error function, namely

$$erf(x) = \frac{2}{\sqrt{\pi}} \int_0^x e^{-\tau^2} d\tau \tag{8}$$

Moreover, in Equation (3), the probability density function $\rho_{\alpha i}$ is characterized by the mean $m_{\alpha i}$, and deviation $\sigma_{\alpha i}$ values

$$m_{\alpha i} = t_{\alpha i} + \sqrt{z}\, \sigma_{\alpha i}, \quad \textit{and} \quad \sigma_{\alpha i} = \sqrt{z}/\lambda_{\alpha i} \tag{9}$$

The first expression in Equation (9) is a restriction between the mean and deviation, because the time $t_{\alpha i}$ has no negative value, and therefore, $m_{\alpha i}$ and $\sigma_{\alpha i}$ are not wholly independent.

In summary, the monomer-α conversion function p_α has the domain $0 < t$, is a continuous function, has no negative values $p_\alpha(t) \ge 0$, is a monotonically non-decreasing function $\dot{p}_\alpha(t) \ge 0$, and has the limit $p_\alpha(t) \to 100\%$ at the end of the polymerization experiment, *i.e.*, at $t \to \infty$. The adjustment parameters are in the set $\mathcal{A}_\alpha = \{w_{\alpha 1}, m_{\alpha 1}, m_{\alpha 2}, \sigma_{\alpha 1}, \sigma_{\alpha 2}\}$, and are determined by minimizing the mean square deviation between the experimental data and results from the conversion function.

2.3 Results

The experimental data of the conversion percentage of monomers corresponds to a ternary mixture, which is formed by the AM, VP, and VBIM monomers with the following initial molar distribution: 35:35:30. The mean square deviation between the conversion function and experimental data is

$$\varepsilon_\alpha^2 = \frac{1}{M} \sum_{i=1}^{M} \left(p_\alpha(t_i) - p_{\alpha i}^{(\text{exp})} \right)^2 \tag{10}$$

where $p_{\alpha i}^{(\text{exp})}$ is the monomer-α conversion data derived from the polymerization experiment at time t, meanwhile $p_\alpha(t_i)$ is Equation (6) evaluated at time t_i. With this target function, Equation (10), the set $\mathcal{A}_\alpha$ is derived from a minimization procedure, and the values of the resulting parameters are displayed in Table 1.

Table 1. Parameters of Equation (1) computed to fit the experimental data. The last column corresponds to the resulting values of the mean square deviation, Equation (10).

α	$\mathbf{w}_{\alpha\mathbf{1}}$	$\mathbf{m}_{\alpha\mathbf{1}}$ [min]	$\sigma_{\alpha\mathbf{1}}$ [min]	$\mathbf{m}_{\alpha\mathbf{2}}$ [min]	$\sigma_{\alpha\mathbf{2}}$ [min]	ε_α
AM	0.4544	17.5482	11.0984	198.885	59.6463	0.0157
VP	0.4331	23.0033	14.5486	232.390	94.3888	0.0162
VBIM	0.2909	42.5098	25.3175	306.502	150.521	0.0083

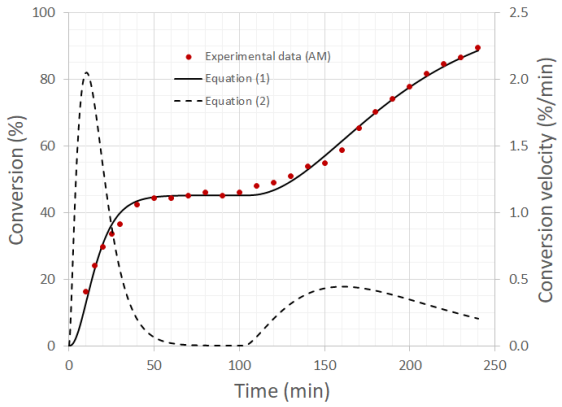

Fig. 1. AM monomer molar conversion as a function of time in the ternary chemical reaction (solid curve and red circles). The dashed curve corresponds to the conversion velocity and its scale is on the left.

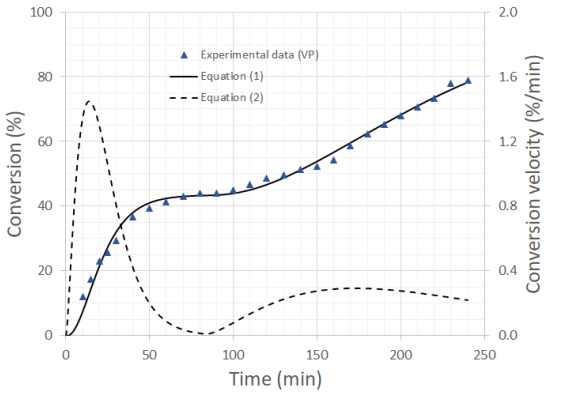

Fig. 2. VP monomer molar conversion as a function of time in the ternary chemical reaction (solid curve and blue triangles). The dashed curve corresponds to the conversion velocity and its scale is on the left.

The results obtained with Equation (1) are shown in Figure 1 with the black solid line for the AM case. The corresponding conversion experimental data are the red-filled circle symbols. In this case, the AM monomers have a violent chemical reaction, and therefore, the maximum conversion velocity is practically reached at the beginning of the chemical reaction. However, after this first stage, perhaps the charge of the polymers, and/or the polymer steric effect work(s) against the aggregation of new monomers into the polymer chains, and therefore, the conversion of monomers starts to decrease. At this stage, the conversion velocity reaches its first minimum (see the dashed curve in Figure 1). At the third stage, the repulsion to the AM monomer decreases, and its aggregation to the polymer structures increases again. As a result, the conversion velocity achieves a second maximum. After this stage, the monomer number begins now to decrease, and the conversion velocity starts to decrease to zero. Finally, AM monomers are fully added to the polymers.

In Figure 2, experimental data of the VP monomer are shown with blue-filled triangle symbols, the results obtained with Equation (1) are shown with the black solid curve, and the conversion velocity results computed with Equation (1) are displayed with the dashed curve. The chemical reaction of the VP monomer is like in the AM monomer case, but the VP monomer conversion is less than that of AM monomers (see Figures 1 and 2). In other words, VP monomers take a little more time to complete 100% of polymerization than AM monomers. Since the chemical structure of each monomer is decisive in the reactivity, most reported studies indicate that AM has high reactivity (Bazaldua, 2023), and the reaction conditions (temperature, solvent, temperature, initiator, etc.) play an important role in this capacity.

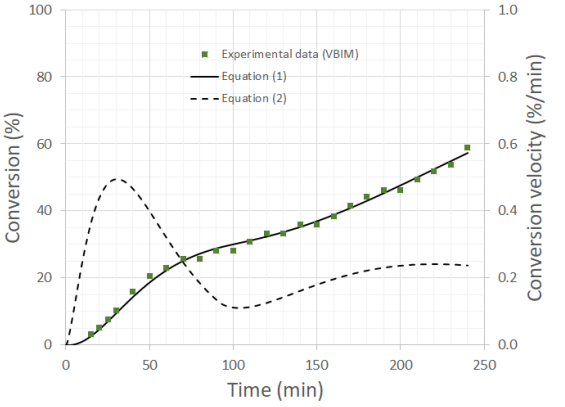

Fig. 3. VBIM monomer molar conversion as a function of time in the ternary chemical reaction (solid curve and green squares). The dashed curve corresponds to the conversion velocity and its scale is on the left.

In Figure 3, the VBIM monomer experimental data are shown with green-filled square symbols, the results derived from Equation (1) are shown with the solid curve, and the conversion velocity results derived from Equation (2) are shown with the dashed curve. The VBIM monomer conversion results agree with the experimental data, but the behavior pattern is not like in the previous cases. In this one, the VBIM monomer is characterized by a slow chemical reaction, and in fact, the conversion velocity reached its maximum at 30 min. After that, the monomer conversion is quite like in the other cases, but the conversion value is always below the others, and therefore, these monomers are the last to complete the polymerization reaction. In this case, it must be considered that VBIM is a cationic monomer that has a charge distribution on the chemical structure, affecting the electrostatic, attractive and repulsion forces between the ionic comonomers (Bazaldua, 2023).

In summary, the conversion velocity, in Equation (2), is modeled with the bimodal probability density

from the Gamma distribution. At least from this flask polymerization experiment on laboratory scale, it was concluded that Equations (1) and (2) described the conversion data. In the next section, the conversion functions will be used to define the next polymerization experiment with dosage on micro-plant scale, *i.e.*, with 1 L to 5 L size.

3 Monomer molar conversion (with dosage)

3.1 Dosage of chemical reactants

The simplest chemical dosage is obtained by using a ramp function, namely

$$f_\alpha(t) = \begin{cases} 0 & t \le 0 \\ \frac{t}{T_\alpha} & 0 < t \le T_\alpha \\ 1 & T_\alpha < t \end{cases} \tag{11}$$

where T_α is the time for adding all the monomers-α to the mixture in the flask. In the same way, $f_\alpha(t)$ is the fraction of the monomers (added to the system) at time t, and no more monomers are added beyond time T_α.

In this work, the monomer molar conversion (with dosage) is approached with the next convolution

$$\mathcal{P}_\alpha(t) = \int_0^t \dot{f}_\alpha(\tau)\; p_\alpha\left(\omega(t-\tau)\right)\; d\tau \tag{12}$$

where $\dot{f}_\alpha$ is the addition velocity. The monomer-α conversion percentage $\mathcal{P}_\alpha$ is considered a superposition of the partial monomer-α conversion percentage p_α, but at different initial times. However, the p_α argument is scaled by the parameter ω whose value is defined from the condition $\mathcal{P}_\alpha\left(0.7\; T_{\text{exp}}\right) \ge 98\%$, where T_{exp} is the experiment duration. In this way, ω depends implicitly on the mixture size. Equation (12) connects the lab and micro-plant scales, however, the interactions between fresh monomers, product (polymers), and initiator molecules are not included.

In general, the $\mathcal{P}_\alpha$ behavior is like p_α, *i.e.* $\mathcal{P}_\alpha$ has the domain $0 \le t$; is a continuous function; has no negative values $\mathcal{P}_\alpha(t) \ge 0$; is a monotonically non-decreasing function $\dot{\mathcal{P}}_\alpha(t) \ge 0$; and has the limit $\mathcal{P}_\alpha(t) \to 100\%$ at $t \to \infty$. However, it has an additional property, namely

$$\lim_{T_\alpha \to 0} \mathcal{P}_\alpha(t) = \; p_\alpha(\omega t) \tag{13}$$

The equation for $\mathcal{P}_\alpha$ is derived from Equations (6), (11), and (12). The result is

$$\mathcal{P}_\alpha(t) = \begin{cases} 0 & t < 0; \\ \mathbb{P}_\alpha(\omega t) & 0 \le t < T_\alpha; \\ \mathbb{P}_\alpha(\omega t) - \mathbb{P}_\alpha\left(\omega(t - T_\alpha)\right) & T_\alpha \le t. \end{cases} \tag{14}$$

where the function $\mathbb{P}_\alpha$ is

$$\mathbb{P}_\alpha(t) = \frac{100\%}{\omega T_\alpha} \sum_{i=1}^{N} \frac{\omega_{\alpha i}}{\lambda_{\alpha i}} \left(\left(u_{\alpha i} - \frac{5}{2} \right) erf\left(\sqrt{u_{\alpha i}} \right) + \sqrt{\frac{u_{\alpha i}}{\pi}} \left(\frac{4}{3} u_{\alpha i} + 5 \right) e^{-u_{\alpha i}} \right). \tag{15}$$

Now, by considering the next function

$$\delta^2 = \left\langle \sum_{\alpha < \beta} \frac{1}{T_{\text{exp}}} \int_0^{T_{\text{exp}}} \left(\mathcal{P}_\alpha(\tau) - \mathcal{P}_\beta(\tau) \right)^2 d\tau \right\rangle \tag{16}$$

where $\langle \ldots \rangle$ is the mean value of all integrals of distinct pairs $(\alpha,\ \beta)$. In this way, the function δ is the mean quadratic deviation between pairs of functions $\mathcal{P}_\alpha$ and $\mathcal{P}_\beta$. If δ is at an extreme point (minimum), then all conversion functions are similar. In other words, $\mathcal{P}_\alpha$ *"follows"* to $\mathcal{P}_\beta$. In this case, perhaps, the final product (the polymers) could have a homogeneous monomer distribution in the polymer structure, and the total number of residual monomers (without chemical reaction) could be a minimum at the end of the experiment. The dosage time is calculated from equations: $\frac{\partial \delta}{\partial T_\alpha} = 0$. Table 2 shows some results corresponding to values of the experiment duration. The model suggests the following dosage times, namely, $T_{\text{AM}} \approx 240$ *min* and $T_{\text{VP}} \approx 200$ *min* for the experiment duration $T_{\text{exp}} \approx 350$ *min*, as an example.

Table 2. Results obtained with the model. The parameter ω, dosage time T_α, and deviation δ are functions of the experiment duration: T_{exp}.

$\mathbf{T}_{\text{exp}}$ [min]	ω	$\mathbf{T}_{\mathbf{AM}}$ [min]	$\mathbf{T}_{\mathbf{VP}}$ [min]	$\mathbf{T}_{\mathbf{VBIM}}$ [min]	δ
250	5.9261	169.27	146.19	121.04	1.7284
300	4.8526	201.81	174.17	143.25	1.7151
350	4.2420	237.02	204.98	169.75	1.7297
400	3.7270	271.32	234.66	194.61	1.7324
450	3.3274	305.74	264.45	219.66	1.7351

3.2 Micro-plant scale

Reactions at micro-plant level were performed in 1 *L* and 5 *L* glass reactors from Chemglass at 50ºC. Reactions were carried out in a reactor equipped with mechanical stirring and double stirrer: the upper impeller is a PTFE four-blade stirrer with a 60° angle, and the lower impeller is a high-viscosity PTFE stirrer with four blades. The benchtop reactor system comprises a jacketed borosilicate glass vessel (type I, class A, meeting ASTM E438 specification) and oil circulation system. The molar rates of the monomers were 35:35:30 for AM:VP:VBIM, respectively. Initially, the slowest-to-react monomer VBIM was introduced into the reactor; then, the other two monomers were introduced adjusting the adding times according to the theoretical results. The steps of the two processes were the following:

1. 50% of the total reaction volume was introduced into the reactor containing the monomer VBIM with constant stirring at 70 *rpm*.
2. Vacuum was made in the reactor for 1 h to eliminate all the oxygen contained in the water solution; then, nitrogen was introduced and maintained during the reaction.
3. Monomers AM and VP were dissolved separately in the laboratory and deareated for 1 h at 20% of the total reaction volume. Initiator *V*50 was dissolved and deareated for 1 h in the remaining 10% of the volume.
4. The reactor temperature was set at 50 ºC.
5. By means of peristaltic pumps, monomers AM and VP were pumped at different flow rates to dosage them at 240 *min* and 200 *min*, respectively, while *V*50 was introduced for 200 *min*.

3.3 Results

Figure 4 shows the ^{1}H-NMR spectra corresponding to the $1-L$ reaction. At zero time there are no signals of the monomers AM and VP, which were added to the reactor at different speeds. As the reaction time progressed, the signals of these monomers increased up to a time of 75 *min*, and then, began to decrease. At 200 *min*, the signals of monomers AM and VP are almost imperceptible, which indicates that they reacted as they were added until being completely consumed. After 240 *min* of reaction, only very weak signals of the monomer VBIM remained.

Figure 5 shows the monomer conversion of the reacting mixture, where it is appreciated that the three monomers reacted at practically the same rates, meanwhile the solid curves are the prediction of the model; all the curves are similar between them and

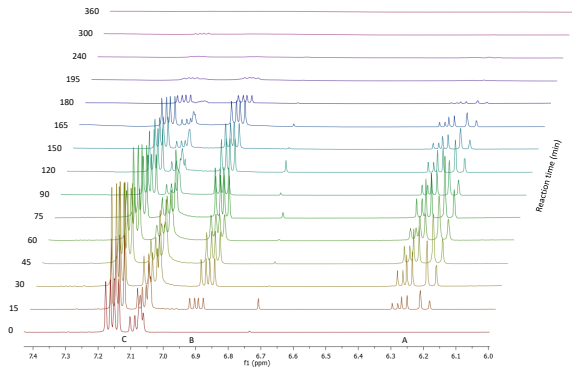

Figure 4. ^{1}H-NMR spectra of the 1-L reaction. A multiplet in the interval ranging from 7.08 to 7.18 *ppm*, marked with the letter "C", corresponds to a proton of the vinyl group of the VBIM monomer; the quadruplet at 6.92 *ppm*, marked with the letter "B", belongs to one of the VP vinyl protons; and finally, a multiplet in the 6.20-6.29 *ppm* region, marked with the letter "A", corresponds to two vinyl protons of the monomer AM.

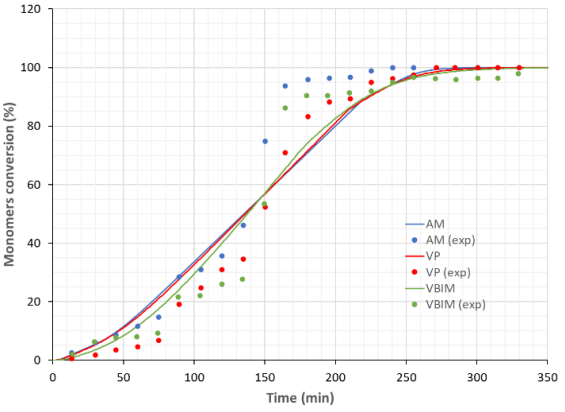

Figure 5. Monomer conversion as a function of time in the 1 *L* reactor. Dots represent the experimental monomer conversion, meanwhile the solid curves correspond to $\mathcal{P}_\alpha$ predicted by the model with the dosage times $T_{\mathrm{AM}} \approx 240$ *min*, $T_{\mathrm{VP}} \approx 200$ *min*, for the experiment duration $T_{\mathrm{exp}} \approx 350$ *min* (see Table 2). The experiment temperature was 50ºC.

qualitatively describe the experimental data. As for the temperature, it rose as the reaction progressed, having a maximum delta of 4ºC, but the cooling water was maintained at no more than 51ºC.

For the reaction at 5 *L*, the reaction conditions were the same as for the case of the reaction at 1 *L*. The ^{1}H-NMR analysis is presented in Figure 6. The developed reaction is like the one at 1 *L* volume and could be considered completed after 240 *min*. In this reaction, the temperature of the internal reaction mixture and torque of the stirring propellant were measured. The increase in torque gives an idea of the increased viscosity of the solution. Figure 7 shows these measurements as the reaction progressed. A moderate increase in torque

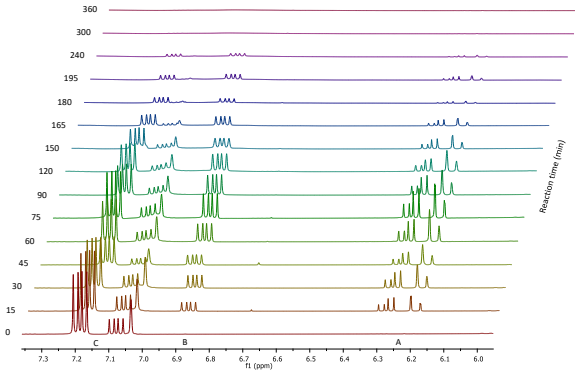

Figure 6. ^{1}H-NMR spectra of the reaction at 5 *L*. A multiplet in the interval ranging from 7.08 to 7.18 *ppm*, marked with the letter "C", corresponds to a proton of the vinyl group of the VBIM monomer; the quadruplet at 6.92 *ppm*, marked with the letter "B", belongs to one of the VP vinyl protons; and finally, a multiplet in the 6.20-6.29 *ppm* region, marked with the letter "A", corresponds to two vinyl protons of the monomer AM.

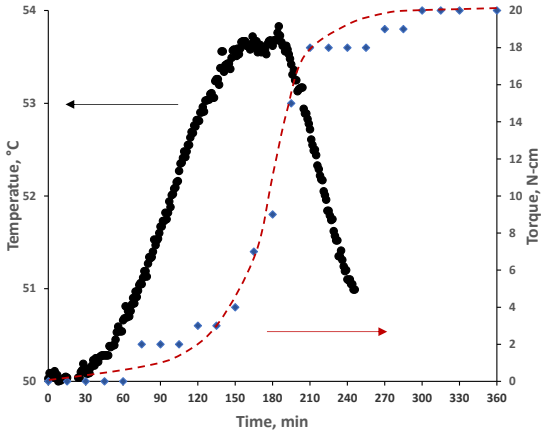

Figure 7. Temperature and torque as functions of time, 5 *L* reaction.

was observed from the first reaction minutes, while a continuous increase in temperature took place to reach an increment of 4ºC from the initial temperature. A sudden increase in torque between 150 *min* and 200 *min* occurred, which coincided with the maximum reached temperature. Finally, the torque tended to stabilize while temperature dropped with the reactor cooling jacket.

The results show the monomer conversion at different rates and any of them reached complete conversion in 240 *min* of reaction, while terpolymerizations on micro-plant scale with adjusted dosage were carried out at similar rates of the three monomers, all reaching 100% conversion close to 240 *min* of reaction time. The improvement in compositions from batch reactor to microscale reactions is evident from Table 3. In the first case, AM was the fastest to react, and this fact prevented it

Table 3. Composition of the final terpolymers obtained by ^{1}H-NMR.

	AM	VP	VBIM
	[*mol%*]	[*mol%*]	[*mol%*]
Batch reaction	16.7	34.8	48.5
1 L reaction	38.8	34.8	26.4
5 L reaction	39.0	34.0	27.0

from integrating into the terpolymeric network. When the conversion of AM followed that of VP and VBIM, its integration improved remarkably.

Finally, this methodology was used to describe the experimental data for the lab and micro-plant scales, where both were connected using Equation (12) and a uniform monomer dosage, however, if calorimetry data were considered, this methodology could be updated and extended to the industrial scale.

Conclusion

Two micro-plant reactions revealed that three monomers (AM, VP and VBIM) were consumed similarly. Since they have different reaction rates, derived from observations of conversion plots, they become minimal by using dosages at different speeds. The slowest monomer (VBIM) was first put into the reactor to be completely available to react during all the reaction time; then, the fastest monomer (AM) was added at lower speed than that of monomer VP so that it could be better distributed in the terpolymer chains and react in a more similar way than the other two monomers.

Based on laboratory polymerization reactions, the dosage rate of monomers was estimated so that their integration into the polymer chains was carried out more homogeneously. Theoretical calculations were performed using Equation (1), reproducing the experimental data with very good fitting. The obtained dosage rates were used to define the experiment on micro-plant scale. From this experiment, the consumption of the reagents occurred at similar rates. The increase in the torque of the stirring arrow and temperature coincided with the accelerated conversion of the monomers between 150 *min* and 200 *min* of reaction.

In this model, the fundamental idea is that the fastest reactive monomers "*follow*" the slowest ones in the system. Under this assumption, the dosage rate of monomers in a polymerization reaction was established.

Acknowledgements

The present study was supported by Instituto Mexicano del Petróleo through projects D.62028 and D62013.

References

Abramowitz M., Stegun, I.A. (1972). *Handbook of mathematical functions*, Dover publication, NY, USA. ISBN-13: 978-0486612720

Bailey B., Crabtree M., Tyrie J., Elphick J., Kuchuk F., Romano C., Roodhart L., (2000). Review on the Estimating the Effective Way for Managing the Produced Water: Case Study. *Oilfield Rev.*, **12** (1), 30-51. www.doi.org/10.4236/ojmh.2021.112002

Barner-Kowollik C., Beuermann S., Buback M., Hutchinson R.A., Junkers T., Kattner H., Manders B., Nikitin A.N., Russell G.T., van Herk A.M., (2017). Critically Evaluated Rate Coefficients in Radical Polymerization. Propagation Rate Coefficients for Vinyl Acetate in Bulk, *Macromol. Chem. Phys*., **218** (1), 1600357. www.doi.org/10.1002/macp.201600357

Bazaldua-Domínguez M., Vega-Paz A., Likhanova N.V., Martínez-Palou R., Guzmán-Lucero D., (2023). In-situ ^{1}H NMR measurements of reactivity ratios and thermal properties for copolymerization of N-vinylpyrrolidone and 1-vinyl-3-butylimidazolium bromide, *Mater. Today Commun*., **35**, 105709. www.doi.org/10.1016/j.mtcomm.2023.105709

Buback M., (1990). Free-radical polymerization up to high conversion. A general kinetic treatment, *Makromol. Chem*., **191** (7), 1575-1587. www.doi.org/10.1002/macp.1990.021910710

Buback M., Hutchinson R.A., Lacík I., (2023). Radical polymerization kinetics of water-soluble monomers, *Prog. Polym. Sci*., **138**, 101645. http://www.doi.org/10.1016/j.progpolymsci.2022.101645

Carraher C.E., (2013). *Carraher's Polymer Chemistry*, CRC Press, NY, USA. http://www.doi.org/10.1201/9781315116600

Cortés J.A., Puig J.E., Morales J.A., Mendizábal E., (2011). Hidrogeles nanoestructurados termosensibles sintetizados mediante polimerización en microemulsión inversa. *Revista Mexicana de Ingeniería Quím*ica, **10** (3), 513–520.

Hutchinson R. A., Beuermann S., Paquet D. A., McMinn J. H., Jackson C., (1998). Determination of Free-Radical Propagation Rate Coefficients for Cycloalkyl and Functional Methacrylates by Pulsed-Laser Polymerization, *Macromolecules*, **31** (5), 1542-1547. http://www.doi.org/10.1021/ma971307u

Jaeger W., Bohrisch J., Laschewsky A., (2010). Synthetic polymers with quaternary nitrogen atoms: Synthesis and structure of the most used type of cationic polyelectrolytes, *Prog. Polym. Sci.*, **35** (5), 511-577. http://www.doi.org/10.1016/j.progpolymsci.2010.01.002

López-Badillo, M., Velasco-Hernández, M., García-Castro, M., Aranda-García R., Galicia-Aguilar J., Guevara-Espinosa M., Carreón-Rodríguez V. (2020). Obtaining kinetic parameters of polyamide imide reaction. *Revista Mexicana de Ingeniería Química, **19**, Cat606.*

Mark J.E., (1999). *Polymer Data Handbook*, Oxford University Press, USA. ISBN: 9780195181012

Martínez-Vázquez N., Antonio-Cruz R. del C., Álvarez-Castillo A., Mendoza-Martinez A., Morales-Cepeda A. B., (2007). Swelling kinetic of hydrogels from methyl cellulose and poly(acrylamide). *Revista Mexicana de Ingeniería Química*, **6** (3), 337–345.

Meyer T., (2003). Scale-Up of Polymerization Process: A Practical Example, *Org. Process Res. Dev*., **7** (3), 297-302. www.doi.org/10.1021/op025605p

Ohara T., Sato T., Shimizu N., Prescher G., Schwind H., Weiberg O., Marten K., Greim H., (2011). *Ullmann's Encyclopedia of Industrial Chemistry*, DOI: www.doi.org/10.1002/14356007 .

Palomeque-Santiago J. F., Vega-Paz A., Likhanova N. V., Guzmán-Lucero D., Guevara-Rodríguez F. de J., (2022). Effect of Ionic Strength on the Polymerization of Acrylamide, N-Vinylpyrrolidone and Vinylbenzyl trimethylammonium chloride, *Chemistry Select*, **7** (20), e202103641. www.doi.org/10.1002/slct.202103641

Preusser C., Chovancová A., Lacík I., Hutchinson R.A., (2016). Modeling the Radical Batch Homopolymerization of Acrylamide in Aqueous Solution, *Macromol. React. Eng*., **10** (5), 490-501. www.doi.org/10.1002/mren.201500076

Ray B., Mandal B.M., (1999). Dispersion polymerization of acrylamide: Part II. 2,2-Azobisisobutyronitrile initiator, *J. Polym.*

Sci. A Polym. Chem., **37** (4), 493-499. http://www.doi.org/10.1002/(SICI)1099-0518(19990215)37:4%3c493::AID-POLA13%3e3.0.CO;2-Y

Santanakrishnan S., Tang L., Hutchinson R.A., Stach M., Lacík I., Schrooten J., Hesse P., Buback M., (2010). Kinetics and Modeling of Batch and Semibatch Aqueous-Phase NVP Free-Radical Polymerization, *Macromol. React. Eng.*, **4** (8), 499-509. www.doi.org/10.1002/mren.201000007

Teleshov E.N., Bune E.V., Gromov V. F., (1994). Characteristic features of the radical polymerisation of water-soluble monomers, *Russ. Chem. Rev.*, **63** (3), 507-517. http://www.doi.org/10.1070/RC1994v063n06ABEH000101

Vasile C., Saade H., Torres S., Barrera C., Sánchez J., Garza Y., López R.G., (2015). Effect of pH and Monomer Dosing Rate in the Anionic Polymerization of Ethyl Cyanoacrylate in Semicontinuous Operation, *Int. J. Polym. Sci.*, **2015**, 827059. http://www.doi.org/10.1155/2015/827059

Williams P.A., (2007). *Handbook of Industrial Water-Soluble Polymers*, Wiley-Blackwell, USA.ISBN: 978-1-405-13242-8

Ye Q., He W., Ge X., Jia H., Liu H., Zhang Z., (2002). Formation of monodisperse polyacrylamide particles by radiation-induced dispersion polymerization. I. Synthesis and polymerization kinetics, *J. Appl. Polym. Sci.*, **86** (10), 2567-2573. http://www.doi.org/10.1002/app.11170